

# Feature Preserving Image Smoothing Using a Continuous Mixture of Tensors \*

Özlem Subakan , Bing Jian , Baba C. Vemuri  
Department of CISE  
University of Florida  
{ons,bjian,vemuri}@cise.ufl.edu

C. Eduardo Vallejos  
Department of Horticultural Sciences  
University of Florida  
vallejos@ufl.edu

## Abstract

*Many computer vision and image processing tasks require the preservation of local discontinuities, terminations and bifurcations. Denoising with feature preservation is a challenging task and in this paper, we present a novel technique for preserving complex oriented structures such as junctions and corners present in images. This is achieved in a two stage process namely, (1) All image data are pre-processed to extract local orientation information using a steerable Gabor filter bank. The orientation distribution at each lattice point is then represented by a continuous mixture of Gaussians. The continuous mixture representation can be cast as the Laplace transform of the mixing density over the space of positive definite (covariance) matrices. This mixing density is assumed to be a parameterized distribution, namely, a mixture of Wisharts whose Laplace transform is evaluated in a closed form expression called the Rigaut type function, a scalar-valued function of the parameters of the Wishart distribution. Computation of the weights in the mixture Wisharts is formulated as a sparse deconvolution problem. (2) The feature preserving denoising is then achieved via iterative convolution of the given image data with the Rigaut type function. We present experimental results on noisy data, real 2D images and 3D MRI data acquired from plant roots depicting bifurcating roots. Superior performance of our technique is depicted via comparison to the state-of-the-art anisotropic diffusion filter.*

## 1. Introduction

Image denoising has a fundamental role in early visual information processing. The role has a twofold purpose: 1) removal of noise which obviously hampers the manual interpretation by humans as well as the automated analysis by computers, 2) the completion or enhancement of local discontinuities, terminations and bifurcations while preserving

features. Smoothing techniques have been widely studied in computer vision for many decades. Many of these methods locally smooth the image along one or several directions chosen to favor smoothing along the image contours so that the edges are not destroyed. Yet it is challenging to enhance patterns with multiple orientations.

There is tomes of literature on image smoothing some of which dates back to the 1970's and is based on linear system theory [17]. In the past fifteen years, there has been a flurry of activity in the applied math community to develop feature preserving image smoothing techniques motivated by the work of Perona and Malik [15]. Their work was based on a partial differential equation describing an anisotropic diffusion filter, where the anisotropy was achieved via a scalar-valued function defined on the image gradient field i.e., a scalar diffusivity coefficient. Several anisotropic diffusion filters were developed after this work, most of them addressing more general issues (generalizing the scalar diffusivity to tensor-valued diffusivity etc.) and some addressing mathematical anomalies (leading to a "paradox") in the original formulation. We refer the reader to [1, 18] for details on some of these techniques. It should be noted that none of these methods addressed the issue of preserving features that represented complex local geometries such as X, T or Y junctions. In [2], a junction preserving filtering technique was introduced using a morphological approach. This technique however requires the junctions to be detected prior to smoothing. More recently, Tschumperlé [20] introduced a curvature preserving smoothing and applied it to scalar, vector and tensor-valued images. The results shown are quite impressive for curvature preservation. What is unclear is whether this technique can preserve junctions where the curvature is not defined. Also, such junctions are not representable by rank-2 tensors.

In the context of deriving local orientation information from scalar-valued images that we will use in the first stage of processing, there are several techniques that maybe applied and one of the most popular one is based on application of Gabor filters. Gabor filters are well-known quadrature filters which have been used widely in image

\*This research was in part supported by NIH EB007082 to BCV and by SM CRSP through a grant from the US Agency of International Development to CEV.

processing applications including registration [11], texture segmentation [4, 22] and edge detection. The main advantage of these filters due to their Gaussian envelopes is that they achieve the minimum space-frequency product specified in the uncertainty principle [6]. They are complex valued functions obtained by modulating Gaussian functions where modulating factor is complex exponential. They are tunable to any desired frequency. Such tuning is particularly useful in capturing any locally predominant orientations present in an image. One of the key drawbacks of Gabor representations is the size of the filter bank one needs in order to acquire useful information. This drawback may be overcome by using steerable filters. Steerable filters provide an efficient platform to synthesize filters of desired orientations from linear combinations of a set of basis filters, allowing one to adaptively “steer” a filter to any orientation and to determine the filter output as a function of orientation [5]. Several frameworks have been presented to find the conditions under which any function steers and also to design a suitable set of basis functions given any arbitrary steerable function; examples include the Lie group theory, SVD approach [19, 13]. More recently Kalliomaki and Lampinen [7] present approximate steerability of Gabor filters in 2D for pattern recognition purposes. In this paper we formulate 3D steerable Gabor filters and exploit them to extract orientation information required in the first stage of the presented approach for junction preserving smoothing.

In this paper, we propose an efficient two-stage “tensor-driven” process. The first stage includes the extraction of local orientation information using steerable Gabor filters applied along several orientations. The second stage involves iterative local convolution at each lattice point with a continuous mixture of Gaussians where the mixing distribution is the mixture of Wisharts whose weights were obtained in the first stage. Several experimental results on real data are shown to depict the performance of our approach in junction preserving image denoising.

The remainder of this paper is structured in the following way: We expand on the steerable Gabor filters in Section 2. Continuous mixture model is presented in Section 3. Then in Section 4, we present experimental results on synthetic images and real data consisting of MRI data acquired from plant roots depicting bifurcating roots. Lastly, we summarize our contributions.

## 2. Local Orientation Representation

Edges, junctions and other transients are the key features that make up an image. In order to afford denoising while preserving these features, we exploit the local orientation information obtained by Gabor filtering the images. Gabor filters are well-known oriented filters which achieve the lower limit of joint uncertainty in spatial and frequency domains [6]. In this sense they are optimal in terms of space-

frequency localization. They have the advantage of being tunable to any frequency or orientation and they can form a relatively good approximation of a wavelet frame. Their use for the analysis of local image structure has been explored widely; [5] is a good example of this.

### 2.1. Steerable Gabor filters

The complex 3D oriented Gabor filter with a non-spherical Gaussian envelope function has the following generic form:

$$f(\boldsymbol{\xi}; \boldsymbol{\mu}, \boldsymbol{\Sigma}, \mathbf{R}_\nu) = \frac{|\boldsymbol{\mu}|^2}{\sqrt{\det \boldsymbol{\Sigma}}} \exp\left(-\frac{|\boldsymbol{\mu}|^2}{2} (\mathbf{R}_\nu^T \boldsymbol{\xi})^T \boldsymbol{\Sigma}^{-1} \mathbf{R}_\nu^T \boldsymbol{\xi}\right) \exp(i\boldsymbol{\mu}^T \mathbf{R}_\nu \boldsymbol{\xi}) \quad (1)$$

where  $\boldsymbol{\xi} = [x, y, z]^T$  is the spatial coordinate vector,  $\boldsymbol{\mu} = [f_c \ 0 \ 0]^T$  is the wave vector which determines the center frequency of the filter,  $\boldsymbol{\Sigma}$  is a diagonal covariance matrix with diagonal entries  $\sigma_x^2 > \sigma_y^2 = \sigma_z^2$  that determines the frequency bandwidths along the axes in Cartesian coordinates and  $\mathbf{R}_\nu$  is a 3D rotation matrix whose first column is a unit vector  $\boldsymbol{\nu}$ . Note that the resulting filter has a constant template ellipsoid determined by  $\boldsymbol{\Sigma}$  and is oriented along the orientation determined by  $\boldsymbol{\nu}$ . Therefore  $f(\boldsymbol{\xi}; \boldsymbol{\mu}, \boldsymbol{\Sigma}, \mathbf{R}_\nu)$  is a complex sinusoid modulated by a 3D Gaussian function  $N(0, |\boldsymbol{\mu}|^2 \mathbf{R}_\nu^T \boldsymbol{\Sigma} \mathbf{R}_\nu)$  with some normalization factor. The term  $\frac{|\boldsymbol{\mu}|^2}{|\boldsymbol{\Sigma}|^{1/2}}$  in Eq. (1) compensates for the frequency related decrease in the power spectrum of images [3]. Since the Fourier transform of a Gaussian function is again a Gaussian function and rotations in the spatial domain correspond to rotations in the frequency domain, the frequency response of the complex Gabor function can be given by a single Gaussian function  $N(\mathbf{R}_\nu^T \boldsymbol{\mu}, \mathbf{R}_\nu^T \boldsymbol{\Sigma}^{-1} \mathbf{R}_\nu)$  with some normalization term. Hence the Fourier transforms of the real and imaginary parts of the complex filter are as follows:

$$\mathcal{F}(\text{Real}\{f\}) \propto N(\mathbf{R}_\nu^T \boldsymbol{\mu}, \mathbf{R}_\nu^T \boldsymbol{\Sigma}^{-1} \mathbf{R}_\nu) + N(-\mathbf{R}_\nu^T \boldsymbol{\mu}, \mathbf{R}_\nu^T \boldsymbol{\Sigma}^{-1} \mathbf{R}_\nu) \quad (2)$$

$$\mathcal{F}(\text{Imag}\{f\}) \propto N(\mathbf{R}_\nu^T \boldsymbol{\mu}, \mathbf{R}_\nu^T \boldsymbol{\Sigma}^{-1} \mathbf{R}_\nu) - N(-\mathbf{R}_\nu^T \boldsymbol{\mu}, \mathbf{R}_\nu^T \boldsymbol{\Sigma}^{-1} \mathbf{R}_\nu) \quad (3)$$

Since real and imaginary parts of the complex Gabor function are approximately in quadrature, the amplitude and phase of the signal can be studied independently. The above filters contain a DC component, i.e. their means are nonzero which makes these filters sensitive to the gray level of the image. This can be avoided by subtracting a scaled Gaussian (with a factor of  $\exp(-\frac{\text{trace}(\boldsymbol{\Sigma})}{2})$ ) located at the origin from Eq. (1). The behavior of this type of filter is similar to the original filter. In fact, the effect of the additional term

forcing the DC response of the filter to zero is negligible unless the frequency bandwidths are close to zero. To compute the response of each filter, we employ steerability of 3D Gabor filters which allows arbitrarily oriented 3D Gabor filters to be applied over a continuum of orientations. Following the concept of steerable filters [5], a 3D oriented Gabor filter can be approximated by a linear combination of basis filters as follows:

$$f^\nu(\boldsymbol{\xi}) \approx \sum_{j=1}^N k_j(\nu) g^{\nu_j}(\boldsymbol{\xi}) = \mathbf{k}^T \mathbf{g} \quad (4)$$

where  $\mathbf{g} = \{g_{\nu_1}, g_{\nu_2}, \dots, g_{\nu_N}\}$  denotes a set of basis filters and  $\mathbf{k} = \{k_1(\nu), k_2(\nu), \dots, k_N(\nu)\}$  denotes a set of steering coefficients. We assume that the basis filters share the same shape parameters and center frequency. The maximum likelihood estimate of the optimal steering coefficients  $k$  naturally leads to the  $L_2$  norm as a measure of goodness of the fit. The corresponding quadratic programming (QP) problem minimizing the residual sum of squares  $\min \|f^\nu - \mathbf{k}^T \mathbf{g}\|^2$  can be efficiently solved by solving a linear system  $\mathbf{G} \mathbf{k} = \boldsymbol{\gamma}$  where the matrix  $\mathbf{G}$  and vector  $\boldsymbol{\gamma}$  consist of the inner products of rotated Gabor functions, i.e.  $\mathbf{G}_{i,j} = \langle g^{\nu_i}, g^{\nu_j} \rangle$  and  $\gamma_i = \langle f^\nu, g^{\nu_i} \rangle$ . We formulate the steerable 3D Gabor filters below. First, note that the product of two Gaussian probability distributions is another Gaussian (unnormalized).

$$N(\boldsymbol{\mu}_a, \boldsymbol{\Sigma}_a) \cdot N(\boldsymbol{\mu}_b, \boldsymbol{\Sigma}_b) = z_c N(\boldsymbol{\mu}_c, \boldsymbol{\Sigma}_c) \quad (5)$$

where  $\boldsymbol{\Sigma}_c = (\boldsymbol{\Sigma}_a^{-1} + \boldsymbol{\Sigma}_b^{-1})^{-1}$  and  $\boldsymbol{\mu}_c = \boldsymbol{\Sigma}_c (\boldsymbol{\Sigma}_a^{-1} \boldsymbol{\mu}_a + \boldsymbol{\Sigma}_b^{-1} \boldsymbol{\mu}_b)$  and

$$z_c = |2\pi(\boldsymbol{\Sigma}_a + \boldsymbol{\Sigma}_b)|^{-1/2} \exp\left(-\frac{1}{2}(\boldsymbol{\mu}_a - \boldsymbol{\mu}_b)^T (\boldsymbol{\Sigma}_a + \boldsymbol{\Sigma}_b)^{-1} (\boldsymbol{\mu}_a - \boldsymbol{\mu}_b)\right) \quad (6)$$

So the inner product integral of two Gaussians is  $z_c$ . Using equations (2) and (3) and a symmetry argument, the inner product integral of two even Gabor functions in frequency space is

$$\begin{aligned} & \langle \mathcal{F}(g_1), \mathcal{F}(g_2) \rangle \propto \\ & 2 \int N(\mathbf{R}_{\nu_1}^T \boldsymbol{\mu}, \mathbf{R}_{\nu_1}^T \boldsymbol{\Sigma}^{-1} \mathbf{R}_{\nu_1}) N(\mathbf{R}_{\nu_2}^T \boldsymbol{\mu}, \mathbf{R}_{\nu_2}^T \boldsymbol{\Sigma}^{-1} \mathbf{R}_{\nu_2}) + \\ & 2 \int N(\mathbf{R}_{\nu_1}^T \boldsymbol{\mu}, \mathbf{R}_{\nu_1}^T \boldsymbol{\Sigma}^{-1} \mathbf{R}_{\nu_1}) N(-\mathbf{R}_{\nu_2}^T \boldsymbol{\mu}, \mathbf{R}_{\nu_2}^T \boldsymbol{\Sigma}^{-1} \mathbf{R}_{\nu_2}) \end{aligned}$$

Inner product integral of two odd Gabor functions can be obtained similarly. After computing the inner products, we can solve  $\mathbf{G} \mathbf{k} = \boldsymbol{\gamma}$  for the optimal steering coefficients and then compute the filter for a specific orientation using Eq. (4). All oriented filters are approximated equally well in the sense of  $L^2$ -norm.

### 3. The Mixture of Wisharts Model and Denoising Kernel

We represent the orientation distribution at each lattice point by a continuous mixture of oriented Gaussians. We postulate that at each voxel there is an underlying probability measure associated with the manifold of  $n \times n$  symmetric positive-definite matrices,  $\mathcal{P}_n$  (by default  $\mathcal{P}_3$ ). Let  $f(D)$  be its density function with respect to some carrier measure  $dD$  on  $\mathcal{P}_n$ . Then the orientation energy can be modeled as:

$$S(\boldsymbol{\xi}; \mathbf{g})/S_0 = \int_{\mathcal{P}_n} f(D) \exp[-\mathbf{g}^T D \mathbf{g}] dD, \quad (7)$$

where  $S_0$  is the maximum orientation energy,  $\boldsymbol{\xi}$  encodes the spatial coordinates and  $\mathbf{g}$  is a unit direction vector. Note that Eq. (7) implies a continuous form of mixture model with  $f(D)$  being a mixing density over the components in the mixture.

Since  $\mathbf{g}^T D \mathbf{g}$  in Eq.(7) can be replaced by  $\text{trace}(B D)$  where  $B = \mathbf{g} \mathbf{g}^T$ , the equation (7) can be expressed as the Laplace transform (matrix variable case) [12]:

$$S(\boldsymbol{\xi}; \mathbf{g})/S_0 = \int_{\mathcal{P}_n} \exp(-\text{trace}(B D)) f(D) dD = (\mathcal{L}_f)(B),$$

where  $\mathcal{L}_f$  denotes the Laplace transform of a function  $f$  which takes its argument as symmetric positive definite matrices from  $\mathcal{P}_n$ .

This expression naturally leads to an inverse problem: recovering of a distribution defined on  $\mathcal{P}_n$  that best explains the observed orientation energy  $S(\mathbf{g})$ . This is an ill-posed problem and in general is intractable without prior knowledge of the probabilistic structure. We consider the orientation tensor as random variable (matrix) belonging to some known distribution family, which allows us to model the uncertainty in the orientation tensor estimation. The orientation tensor can be interpreted as the concentration matrix (inverse of the covariance matrix) of the Gaussian distribution in the  $g$ -space. It is a common practice to put a Wishart distribution (see definition below) prior, on the concentration matrix in multivariate analysis. Moreover, in the case of a Wishart distribution, a closed form expression for the Laplace transform exists and leads to a Rigaut-type asymptotic fractal law [16] which has been observed in many biological systems [8] (see explanation below).

**Definition 1** [10] For  $\Sigma \in \mathcal{P}_n$  and for  $p$  in  $(\frac{n-1}{2}, \infty)$ , the Wishart distribution  $\gamma_{p, \Sigma}$  with scale parameter  $\Sigma$  and shape parameter  $p$  is defined as <sup>1</sup>

$$d\gamma_{p, \Sigma}(\mathbf{Y}) = \Gamma_n(p)^{-1} |\mathbf{Y}|^{p-(n+1)/2} |\Sigma|^{-p} e^{-\text{trace}(\Sigma^{-1} \mathbf{Y})} d\mathbf{Y},$$

where  $\Gamma_n$  is the multivariate gamma function and  $|\cdot|$  is the matrix determinant.

<sup>1</sup>Note that the correspondence between this definition and the conventional Wishart distribution  $W_n(p, \Sigma)$  [14] is given simply by  $\gamma_{p/2, 2\Sigma} = W_n(p, \Sigma)$ .

The Wishart distribution  $\gamma_{p,\Sigma}$  is known to have the closed-form Laplace transform:

$$\int e^{-\text{trace}(\Theta Y)} d\gamma_{p,\Sigma}(Y) = (1 + \text{trace}(\Theta \Sigma))^{-p} \quad , \quad (8)$$

where  $(\Theta + \Sigma^{-1}) \in \mathcal{P}_n$ . Let  $f$  in Eq. (7) be the density function of  $\gamma_{p,\Sigma}$  with the expected value  $\hat{D} = p\Sigma$ . We have

$$S(\xi; \mathbf{g}) = S_0 (1 + (\mathbf{g}^T \hat{D} \mathbf{g})/p)^{-p} \quad . \quad (9)$$

The single Wishart distribution model has a drawback in that it cannot resolve the intra-voxel orientational heterogeneity due to the single diffusion maximum in the model. Hence it is natural to use a discrete mixture of Wishart distribution model where the mixing distribution in Eq.(7) is expressed as  $dF = \sum_{i=1}^N w_i d\gamma_{p_i, \Sigma_i}$ . Note that the number of components in mixture,  $N$ , only depends on the discretization resolution and should not be interpreted as the expected number of bifurcations. To estimate the numerical scale of the eigenvalues  $D_i = p\Sigma_i$ , we first assume a single Gaussian model  $S(\xi; \mathbf{g})/S_0 = \exp[-\mathbf{g}^T D \mathbf{g}]$  and then solve the  $D$  using linear regression. The trace of the resulting  $D$  is used as a good estimation for the trace of  $D_i$ . In practice, we further assume that the two smaller eigenvalues of orientation tensors are equal and fix the ratio between the larger eigenvalue and the smaller one. Hence the eigenvalues of  $D_i$  can be determined on a voxel by voxel basis. Furthermore, this rotational symmetry leads to a tessellation where  $N$  unit vectors evenly distributed on the unit sphere are chosen as the principal eigenvectors of  $\Sigma_i$ . For  $K$  measurements with  $\mathbf{g}_j$ , the signal model equation:

$$S(\xi; \mathbf{g}) = S_0 \sum_{i=1}^N w_i (1 + \text{trace}(\mathbf{B} \Sigma_i))^{-p} \quad (10)$$

yields a linear system  $A\mathbf{w} = \mathbf{s}$ , where  $\mathbf{s} = (S(\xi; \mathbf{g})/S_0)$  contains the normalized measurements,  $A$  is the matrix with  $A_{ji} = (1 + \text{trace}(\mathbf{B}_j \Sigma_i))^{-p}$ , and  $\mathbf{w} = (w_i)$  is the weight vector to be estimated. This can be cast as a sparse deconvolution problem formulated in a general form of as,

$$A\mathbf{w} = \mathbf{s} + \eta, \quad (11)$$

where  $\eta$  represents certain noise model. Under the assumption that the measurement errors  $\eta$  are i.i.d. and normally distributed, we use a non-negative least squares (NNLS) minimization to solve for

$$\min \|\mathbf{A}\mathbf{w} - \mathbf{s}\|^2 \quad \text{subject to} \quad \mathbf{w} \geq 0. \quad (12)$$

The most used algorithm for NNLS was developed in [9, Ch.23], which treats the linear inequality constraints using an *active set strategy*. Though the sparsity constraint is not explicitly imposed, the active set strategy tends to find the sparse solution quickly if there exists such one. Additionally, unlike other iterative methods mentioned, the output is

not susceptible to mis-tuning of the input parameters. After  $\mathbf{w}$  is estimated for orientations, we apply an iterative local convolution at each lattice point with the kernel being a continuous mixture of Gaussians formulated as

$$K(\xi, D) = \int_{\mathcal{P}_n} f(D) \exp[-\xi^T D \xi] dD \quad . \quad (13)$$

We assume a discrete mixture of Wishart distribution model for the mixing distribution in Eq.(13) which can be expressed as  $dF = f(D)dD = \sum_{i=1}^N w_i d\gamma_{p_i, \Sigma_i}$ . Using Laplace transform of the Wishart distribution, the kernel model equation is given as

$$K(\xi, D) = \sum_{i=1}^N w_i (1 + \text{trace}((\xi \xi^T D_i)/p))^{-p} \quad . \quad (14)$$

Here weights for Wisharts are obtained by  $\mathbf{w}$  computed in the first stage, namely local orientation estimation. When  $p$  tends to  $\infty$ , this model reduces to a mixture of oriented Gaussians with weight vector  $\mathbf{w}$ .

## 4. Experimental Results

We first test the performance of the methods described in the previous sections on the public domain images<sup>2</sup> with various junctions, corners etc. For comparison purposes, smoothing results obtained using the edge enhancing anisotropic diffusion method in [21] are presented. We fixed the SNR to the value of the best result our method gives and performed the experiments on edge enhancing anisotropic diffusion until that ratio is reached. As it can be seen in Figure 1, our method denoises the noisy clown image while preserving the geometry of the details whereas edge enhancing anisotropic diffusion does not preserve the junctions (see the zoomed-in regions; our method preserves details around the eye while smoothing elsewhere.).

In Figure 4, test results on real 3D MRI data consisting of bean roots are shown. We display the probability map of a bifurcation location using spherical harmonics representation, which is embedded next to the denoising result. This figure illustrates that the orientation distribution is consistent with the computed probability map. Besides, it is evident that our smoothing technique outperforms the competitor; denoising is achieved without losing the essence of the junctions in the roots. We also notice that the filling in of missing directional structures is accomplished in our method.

## 5. Conclusions

In this paper, we have treated the problem of denoising with feature preservation and presented a mathematical model which relates images and probability distributions for positive definite matrix-valued random variables

<sup>2</sup><http://vision.cse.psu.edu/book/testbed/images/>

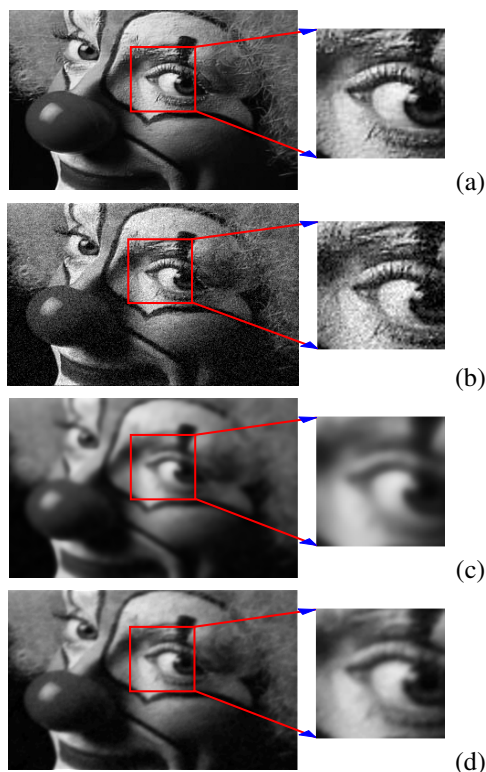


Figure 1. (a) Clown image (of size 320x200 pixels) without noise (b) Noisy image with a gaussian noise of zero mean and 0.07 standard deviation (c) Edge enhancing anisotropic diffusion, local scale  $\sigma = 0.5$ , and 20 iterations (d) Our feature preserving smoothing method in 4 iterations, SNR = 11.7dB

through Laplace transforms. We first extract the local orientation information using steerable Gabor filters and then use these filter responses to compute the weight of each probability density function in a continuous mixture of Gaussians used to represent the geometry of the image function at each lattice point. In order to generate a convolution kernel for smoothing purposes, a continuous mixture of Gaussians with the mixing distribution being a mixture of Wisharts is used locally. We use the closed form expression for the Laplace transform of Wishart distributions. We further note that the traditional mixture of Gaussians model is the limiting case of the orientation energy functional. A sparse deconvolution technique is employed for computation of the weights in the mixture of Wisharts model. The classic non-negative least squares (NNLS) algorithm developed in [9] is most suitable for our deconvolution problem in achieving sparseness and robustness. Finally, the experimental results on several publicly available images and an MRI data set consisting of bifurcating bean roots have shown that the proposed model provides better overall performance than other state-of-the-art techniques for denoising.

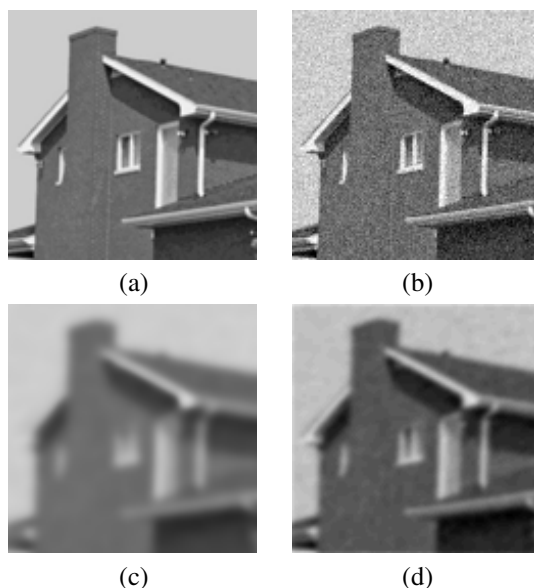


Figure 2. (a) Real image (of size 128x128 pixels) without noise (b) Noisy image with a gaussian noise of zero mean and 0.05 standard deviation (c) Edge enhancing anisotropic diffusion with local scale  $\sigma = 0.5$ , and 20 iterations (d) Our feature preserving smoothing method in 4 iterations, SNR = 12.1dB

## References

- [1] G. Aubert and P. Kornprobst. *Mathematical Problems in Image Processing: Partial Differential Equations and the Calculus of Variations*. Springer-Verlag, 2002.
- [2] V. Caselles, B. Coll, and J. Morel. Junction detection and filtering: A morphological approach. In *ICIP96*, pages 1: 493–496, 1996.
- [3] J. Daugman. Complete discrete 2D gabor transform by neural networks for image analysis and compression. *IEEE Trans. Acoustics, Speech and Signal Processing*, 36:1169–1179, 1988.
- [4] D. F. Dunn, W. E. Higgins, and J. Wakeley. Texture segmentation using 2-d gabor elementary functions. *IEEE Trans. Pattern Anal. Mach. Intell.*, 16(2):130–149, 1994.
- [5] W. T. Freeman and E. H. Adelson. The design and use of steerable filters. *IEEE Trans. Pattern Anal. Mach. Intell.*, 13(9):891–906, 1991.
- [6] G. H. Granlund and H. Knutsson. *Signal Processing for Computer Vision*. Kluwer Academic Publisher, 1995.
- [7] I. Kalliomäki and J. Lampinen. On steerability of gabor-type filters for feature detection. *Pattern Recogn. Lett.*, 28(8):904–911, 2007.
- [8] M. Köpf, C. Corinth, O. Haferkamp, and T. F. Nonnenmacher. Anomalous diffusion of water in biological tissues. *Biophys. J.*, 70:2950–2958, 1996.
- [9] C. Lawson and R. J. Hanson. *Solving Least Squares Problems*. Prentice-Hall, 1974.
- [10] G. Letac and H. Massam. Quadratic and inverse regressions for Wishart distributions. *The Annals of Statistics*, 26(2):573–595, 1998.

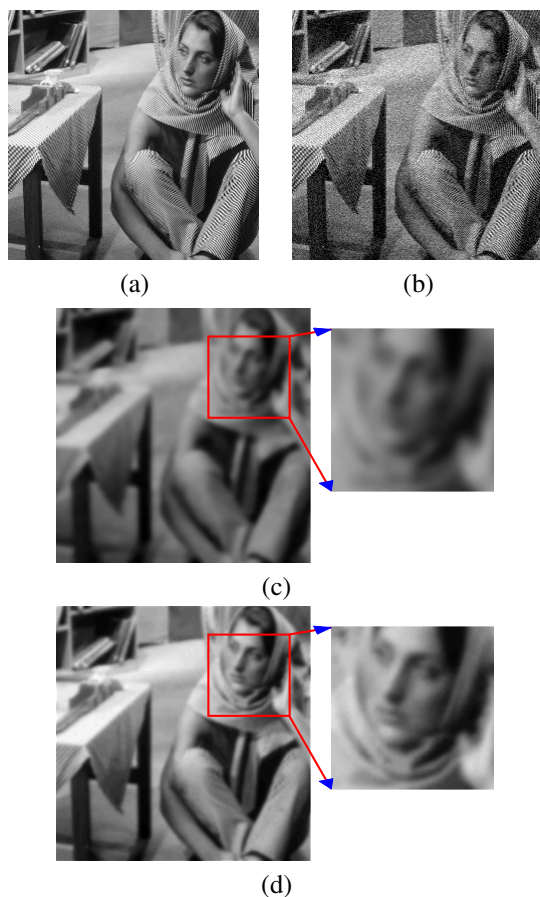


Figure 3. (a) Barbara image (of size 256x256 pixels) without noise (b) Noisy image with a gaussian noise of zero mean and 0.07 standard deviation (c) Edge enhancing anisotropic diffusion with local scale  $\sigma = 0.5$ , and 20 iterations (d) Our feature preserving smoothing method in 4 iterations, SNR = 9.6dB

- [11] J. Liu, B. C. Vemuri, and F. Bova. Efficient multi-modal image registration using local-frequency maps. *Mach. Vision Appl.*, 13(3):149–163, 2002.
- [12] A. M. Mathai. *Jacobians and functions of matrix argument*. World Scientific, 1997.
- [13] M. Michaelis and G. Sommer. A lie group approach to steerable filters. *Pattern Recognition Letters*, 16(11):1165–1174, 1995.
- [14] R. J. Murihead. *Aspects of multivariate statistical theory*. John Wiley & Sons, 1982.
- [15] P. Perona and J. Malik. Scale-space and edge detection using anisotropic diffusion. *IEEE Trans. Pattern Anal. Mach. Intell.*, 12(7):629–639, 1990.
- [16] J. P. Rigaut. An empirical formulation relating boundary lengths to resolution in specimens showing ‘non-ideally fractal’ dimensions. *J Microsc.* 133:41–54, 1984.
- [17] A. Rosenfeld and A. C. Kak. *Digital Picture Processing*. Academic Press, Inc., Orlando, FL, USA, 1982.
- [18] G. Sapiro. *Geometric Partial Differential Equations and Image Analysis*. Cambridge University Press, 2001.

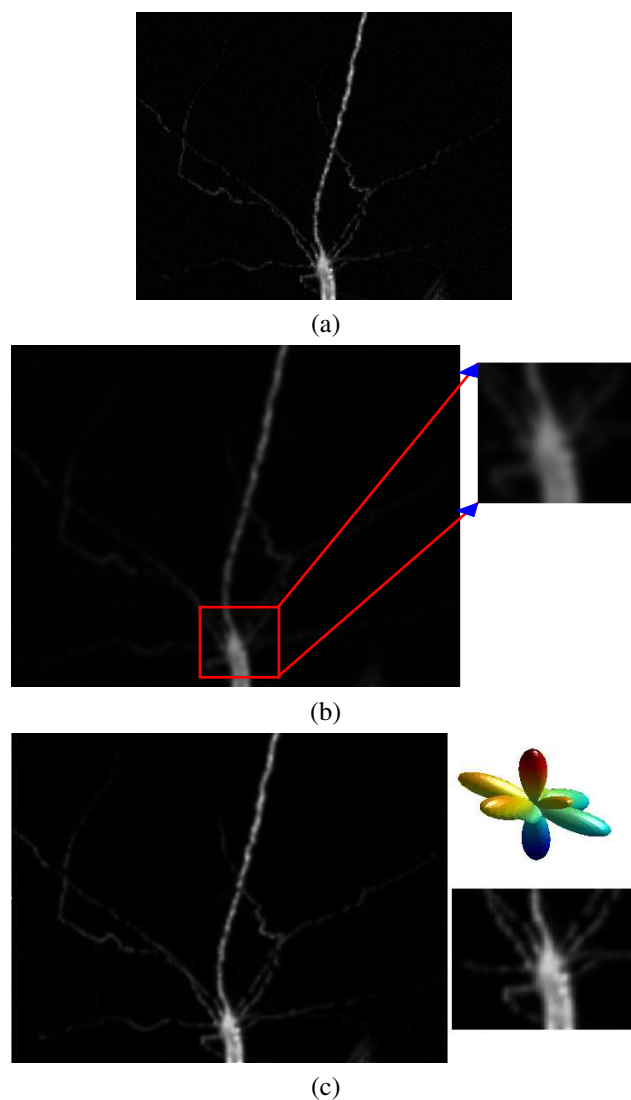


Figure 4. (a) MIP view of real MRI data of a bean root (size 256x256x128 pixels) (b) Edge enhancing anisotropic diffusion with local scale  $\sigma = 0.5$ , and 30 iterations (c) Our feature preserving smoothing method in 4 iterations together with the probability map illustrating the bifurcation structure

- [19] P. C. Teo. *Theory and Applications of Steerable Functions*. PhD thesis, Stanford University, 1998.
- [20] D. Tschumperlé. Fast anisotropic smoothing of multi-valued images using curvature-preserving pde’s. *Int. J. Comput. Vision*, 68(1):65–82, 2006.
- [21] J. Weickert. Coherence-enhancing diffusion filtering. *Int. J. Comput. Vision*, 31(2-3):111–127, 1999.
- [22] T. P. Weldon, W. E. Higgins, and D. F. Dunn. Efficient gabor filter design for texture segmentation. *Pattern Recognition*, 29(12):2005–2015, 1996.